sccer mobility

www.sccer-mobility.ch

In cooperation with the CTI

Energy
Swiss Competence Centers for Energy Research

Schweizerische Eidgenossenschaft
Confédération suisse
Confederazione Svizzera
Confederaziun svizra

Swiss Confederation

Commission for Technology and Innovation CTI

New fuels and new combustion modes: A path to zero emissions / high efficiency mobility systems

LAV Laboratorium für Aerothermochemie und Verbrennungssysteme
Aerothermochemistry and Combustion Systems Laboratory

ETH Eidgenössische Technische Hochschule Zürich
Swiss Federal Institute of Technology Zurich

Computational research

Chemical Energy Carriers for Combustion in Transportation

Despite the continuous development of new technologies the combustion process is still at the basis of most of the energy transformation processes employed in mobility systems.

The continuous study devoted by the research community to the understanding and improvement of the combustion process allowed to match from year to year the always more stringent emission standard regulating the Diesel and gasoline automotive engines.

Moreover, this effort brought light on future and promising paths to further develop the combustion systems and approach the target of highly-efficient/zero emission combustion in mobility systems. In particular:

- The employment of new synthetic fuels that feature specific characteristics
- The development of new combustion strategies

In order to make the best of these two concepts and of their combination, much more understanding is still needed. To pursue this goal at LAV we use different experimental equipments as well as advanced computational methods to understand the process from its fundamentals, until its apllication in real engines.

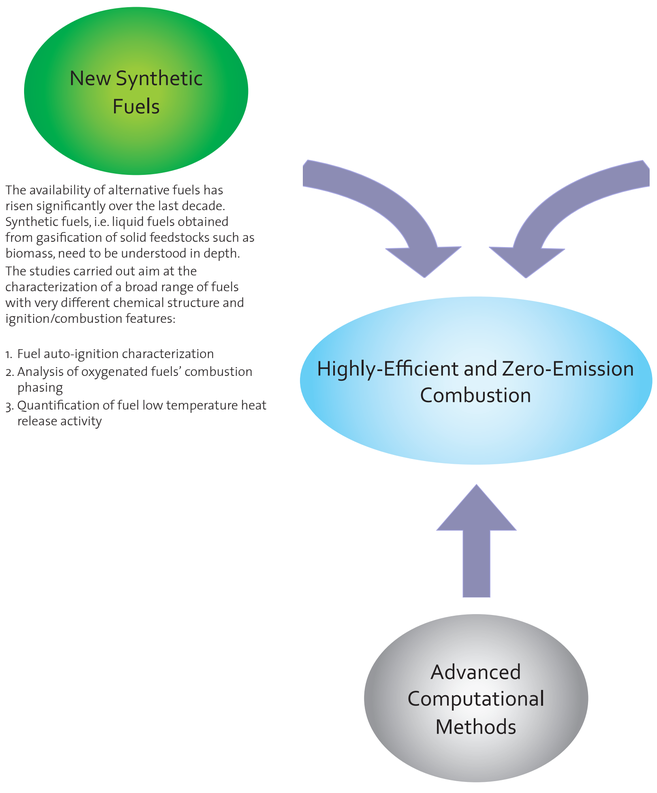

The availability of alternative fuels has risen significantly over the last decade. Synthetic fuels, i.e. liquid fuels obtained from gasification of solid feedstocks such as biomass, need to be understood in depth.
The studies carried out aim at the characterization of a broad range of fuels with very different chemical structure and ignition/combustion features:

1. Fuel auto-ignition characterization
2. Analysis of oxygenated fuels' combustion phasing
3. Quantification of fuel low temperature heat release activity

The development of new combustion strategies in the last years allowed to overcome the traditional problems related to the combustion in reciprocating engines:

- Homogeneous charge compression ignition (HCCI)
- Dual-fuel or Reactivity controlled compression ignition (RCCI)
- Advanced multi-injection strategies

Advanced Computational Methods allow for improved understandings of fundamental flow processes, as for example cyclic variability of the flow field.
The „no-model" approach of DNS makes virtual experiments possible which can provide rich data for subsequent modell development and validation in model based environments such as RANS or LES..
RANS and LES come at considerably reduced computational cost and offer the ability to respect complex geometries found typically in reciprocating piston engines.

Christopher Blomberg blomberg@lav.mavt.ethz.ch
Dimitrios Mitakos mitakos@lav.mavt.ethz.ch
dr. Y. M. Wright wright@lav.mavt.ethz.ch
Prof. K. Boulouchos boulouchos@lav.mavt.ethz.ch

HCCI Combustion with Synthetic Fuels

Introduction

Over the past two decades fuel and transportation industries have witnessed an increasing need to develop more efficient and cleaner engines. This is partially due to drastic world-wide reductions in the regulated limits for pollutant emissions coming from internal combustion engines (ICE) and the steady increase in oil prices. A very promising approach towards in-cylinder emissions reductions and higher engine efficiency is lowering the combustion temperature. This strategy is coined as Low Temperature Combustion (LTC). Homogeneous Charge Compression Ignition (HCCI) belongs to this family of LTC and has been receiving increasing attention from engine manufacturing companies. In brief, this technology tries to blend the advantages of gasoline and diesel engines into one single engine concept.

Many challenges still remain today to make these engines commercially ready. One main challenge is to have complete control over combustion initiation. Fuel chemistry and its kinetics play a dominant role in LTC ignition. To explore the influence of fuel chemistry with simulations, reduced chemical kinetic mechanisms and ignition delay models have gained enormous importance.

At LAV two models have been developed for HCCI combustion:
- A 3-Arrhenius model with the option of using an integrated Cool-Flame model for the full prediction of HCCI ignition delays.
- A 7-step global reaction mechanism to predict ignition delays and characteristic HCCI combustion variables (pressure, temperature, species, etc.).

3-Arrhenius Model

$$\frac{1}{\tau} = \frac{1}{\tau_1 + \tau_2} + \frac{1}{\tau_3}$$

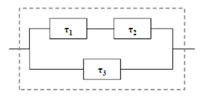

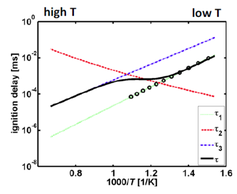

$$\tau_i = A_i \left(\frac{p}{p_{ref}}\right)^{\beta_i} T^{b_i} \exp\left(\frac{T_{A_i}}{T}\right) \varphi^{\gamma_i} \left(\frac{[N_2]}{[O_2]}\right)^{d_i} \exp\left(\frac{[N_2]}{[O_2]}\frac{e_i}{T}\right) \quad \text{for} \quad i = 1,3$$

Global Reaction Mechanism

Reaction	Rate [mol/(cm³.s)]
1. $F + (2x+y)/4\ O_2 \rightarrow y/2\ H_2O + x\ CO$	$R_1 = k_1 [F]^{\gamma} [O_2]^{1.5} (p/p_0)^{c}$
2. $CO + 0.5 O_2 \Leftrightarrow CO_2$	$R_{2+} = k_{2+} [CO][H_2O]^{0.5} [O_2]^{0.25}$ $R_{2-} = k_{2-} [CO_2]$
3. $F + 2O_2 \Leftrightarrow I_1$	$R_{3+} = C_{3+} k_{3+} [F][O_2][M_1] (p/p_0)^{g}$ $R_{3-} = k_{3-} [I_1] (p/p_0)^{h}$
4. $I_1 \rightarrow 2Y$	$R_4 = k_4 [I_1]$
5. $Y + 0.5 F + [(2x+y)/4 - 1] O_2 \rightarrow y/2\ H_2O + x\ CO$	$R_5 = k_5 [F][Y]$
6. $I_1 \rightarrow I_2$	$R_6 = k_6 [I_1]$
7. $I_2 \rightarrow 2Y$	$R_7 = k_7 [I_2][M_2]^{y}$

$k_i = A_i \exp(-E_i/RT)$, $p_0 = 1$ MPa, $[M_1] = p/RT$ and $[M_2] = [F]+[O2]+[I1]+[I2]+[Y]+[CO]$

F	fuel, alkyl radicals, large alkenes and high temperature intermediates (primarily alkenic species)
I_1	alkylperoxy radicals ($RO_2\bullet$) and subsequent hydroperoxy, oxohydroperoxy and ketohydroperoxy alkyl radicals ($ROOH\bullet$, $O_2ROOH\bullet$, $HO_2RO_2H\bullet$)
I_2	mainly H_2O_2, aldehydes and lighter alkenes and ethers formed via the low temperature reaction paths
Y	mainly $HO_2\bullet$ and $OH\bullet$

Results of 3-Arrhenius Model

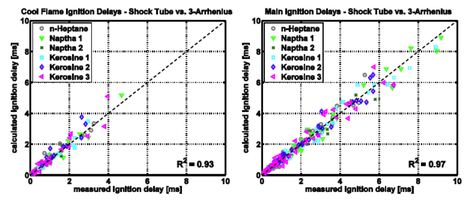

Figure 1 Measured vs. computed cool-flame and main ignition delays of the 3-Arrhenius model for various fuels.

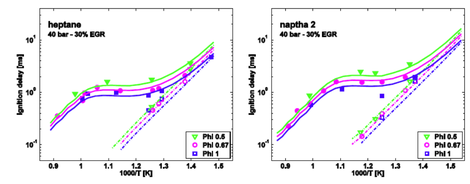

Figure 2 3-Arrhenius curves of measured vs. computed cool-flame and main ignition delays for two exemplary fuels at varying equivalence ratios.

Results of Global Reaction Mecha-

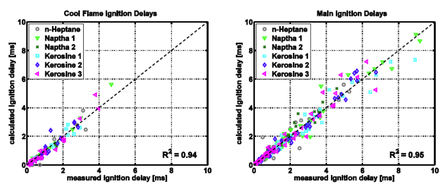

Figure 3 Measured vs. computed cool-flame and main ignition delays of the global reaction model for various fuels.

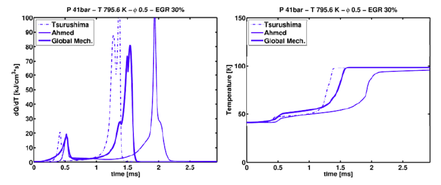

Figure 4 Heat release rate and temperature evolutions for an exemplary shock tube calculation of n-heptane using the global reaction mechanism and two mechanisms from literature.

References

[1] D. Mitakos, et al., "A Cool-Flame Integrated 3-stage-Ignition Model for HCCI Applications," SAE Int. J. Engines, 2013.
[2] A. Vandersickel, et al., "Global Reaction Mechanism for a Selection of Full Boiling Range Gasoline and Kerosene fuels under HCCI Conditions," Combust. Theory Model., 2013.

Funding: FVV, BfE, EV

S. S. Pandurangi* N. Frapolli D. Farrace
M. Bolla Y. M. Wright K. Boulouchos
*<sushpa@lav.mavt.ethz.ch>

DIESEL ENGINES AND SPRAYS
COMBUSTION MODELLING

Influence of EGR on Post-injection Effectiveness in a Heavy-duty Diesel Engine

Introduction

Soot particles emitted by diesel engines are dangerous for the enviroment and for living organisms. Emission legislation around the world is becoming increasingly stringent, demanding better understanding of the physics of soot formation to design countermeasures. One such measure being heavily researched is the addition of a small fuel post-injection. In this numerical study based on data from a heavy-duty research diesel engine [1], we investigate the effect of post-injection on soot evolution and governing processes, and the influence of exhaust gas recirculation on the interaction between post- and main- injections.

Experimental setup [1]

Engine parameters
bore: 140 mm (VH=2.34 L)
CR=11.2(geom.), 16(sim.)
swirl ratio: 0.5
injector: 8 x 0.131 mm
fuel: n-heptane
Measurement techniques
pressure & AHRR
2D natural luminosity
planar LII

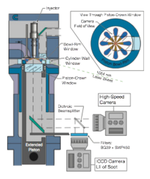

CFD model

CFD computational setup:

- Commercial CFD code STAR-CD [2]
- 2D grid with 1.0 mm mesh size
- k-epsilon turbulence model, wall functions
- Euler-Langrange approach for droplets
- Coditional Moment Closure (CMC) combustion model [3]
- Reduced mechanism for n-heptane [5]
- Two-equations soot model [6]
- Optical-thin soot radiation model [7]
- Soot differential diffusion effects neglected (Le=1)

Soot model: two-equations model [6]

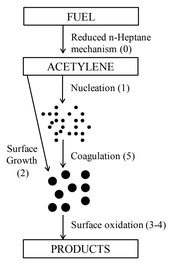

(1) Particle inception:
$C_2H_2 \rightarrow 2C_{(S)} + H_2$
$\dot{\omega}_{INCEP} = 10^4 [C_2H_2] e^{-\frac{21100}{T}}$
(2) Particle surface growth
$C_2H_2 + nC_{(S)} \rightarrow (n+2)C_{(S)} + H_2$
$\dot{\omega}_{SURF\ GROW} = 6 \cdot 10^3 [C_2H_2] e^{-\frac{12100}{T}} \cdot \sqrt{A_{soot}}$
(3) Particle oxidation by O_2:
$C_{(S)} + \frac{1}{2}O_2 \rightarrow CO$
$\dot{\omega}_{OXID_{O_2}} = 10^4 [O_2] e^{-\frac{19000}{T}} \cdot \sqrt{T} \cdot A_{soot}$
(4) Particle oxidation by OH:
$C_{(S)} + OH \rightarrow CO + H$
$\dot{\omega}_{OXID_{OH}} = 0.36 [OH] \cdot \sqrt{T} \cdot A_{soot}$
(5) Particle coagulation:
$nP \rightarrow P_n$
$\dot{\omega}_{COAG} = -3\left(\frac{24R}{\rho_s N_A}\right)^{\frac{1}{2}} \left(\frac{6}{\pi \rho_s}\right)^{\frac{1}{6}} T^{\frac{1}{2}} (\rho Y_S)^{\frac{1}{6}} N_S^{\frac{11}{6}}$

Soot model accouts for simultaneous soot particle inception, surface growth, oxidation by O_2 and OH and coagulation

Solve transport equations for soot mass fraction and soot number density (Le=1):

$$\frac{\partial Q_\alpha}{\partial t} + \langle u_i|\eta\rangle \frac{\partial Q_\alpha}{\partial x_i} = \langle \dot{N}|\eta\rangle \frac{\partial^\alpha Q_\alpha}{\partial \eta^\alpha} + \frac{1}{\bar{\rho}\tilde{P}(\eta)} \frac{\partial}{\partial x_i}\left[(\rho u_i' Y_\alpha'|\eta)\tilde{P}(\eta)\right] = \langle \dot{w}_\alpha|\eta\rangle$$

Source term soot mass fraction:

$$\langle \dot{w}_{Y_S}|\eta\rangle = \langle \dot{w}_{Y_{S,inception}}|\eta\rangle + \langle \dot{w}_{Y_{S,growth}}|\eta\rangle + \langle \dot{w}_{Y_{S,oxidation O_2}}|\eta\rangle + \langle \dot{w}_{Y_{S,oxidation OH}}|\eta\rangle$$

Source term soot number density:

$$\langle \dot{w}_{N_S}|\eta\rangle = \langle \dot{w}_{N_{S,inception}}|\eta\rangle + \langle \dot{w}_{N_{S,coagulation}}|\eta\rangle$$

Governing equations [3]

$$\frac{\partial Q_\alpha}{\partial t} + \langle u_i|\eta\rangle \frac{\partial Q_\alpha}{\partial x_i} = \langle \dot{N}|\eta\rangle \frac{\partial^\alpha Q_\alpha}{\partial \eta^\alpha} + \langle \dot{w}_\alpha|\eta\rangle - \frac{1}{\tilde{\rho}\tilde{P}(\eta)} \frac{\partial}{\partial x_i}\left[(\rho Y_\alpha' u_i'|\eta)\tilde{P}(\eta)\right]$$

$\langle u_i' Y_\alpha'|\eta\rangle = -D_\alpha \frac{\partial Q_\alpha}{\partial x_i}$ **Gradient flux**

$\langle u_i|\eta\rangle = \tilde{u}_i - \frac{D_\alpha}{\tilde{\xi}^2} \frac{\partial \tilde{\xi}}{\partial x_i}(\eta - \tilde{\xi})$ **Linear model for conditional velocity**

$\langle \dot{w}_\alpha|\eta\rangle = \dot{\omega}_\alpha(Q_\alpha, \bar{Q}, \tilde{P})$ **First order closure for source terms**

$\langle N|\eta\rangle = \frac{\tilde{\chi}}{2\left[G(\eta)\tilde{P}(\eta)d\eta\right]^2} \exp\left(-2\left[erf^{-1}(2\eta-1)\right]^2\right)$ **AMC model for scalar dissipation rate**

$\langle \dot{w}_{soot}|\eta\rangle = -4\alpha\sigma_{soot}\left[(T|\eta)^4 - T_{soot}^4\right]$
$\alpha_{soot} = 2370 \frac{1}{mK} \cdot f_{v,soot} \cdot T$ **Optically-thin radiation model [7]**

Interfacing of CFD and CMC code [4]:

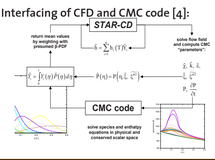

Multiple Injections [8]

Multiple injections using a single total mixture fraction (MFT) as the conditioning scalar.
re-initialisation of conditional temperature and composition in every CMC cell at the time of the first appearance of MF from post injection (MF_2)
constraint: $MF_1 + MF_2 = MFT <= 1.0$

$$\langle T_{Double}|\eta_1, \eta_{Tot}\rangle \equiv \langle T_{\eta_1}|\eta_{Tot}\rangle (H(\eta_{Tot} - \eta_1)) + \langle T_{mix}|\eta_{Tot}\rangle H(\eta_{Tot} - \eta_1)$$

$$\langle T_{New}|\eta_{Tot}\rangle \equiv \int_0^1 \langle T_{Double}|\eta_1, \eta_{Tot}\rangle P_\xi(\eta_1) d\eta_1$$

Number of subsequent injections is not limited with this approach!

Soot formation and oxidation processes

Soot-quantities for single- and post-injection

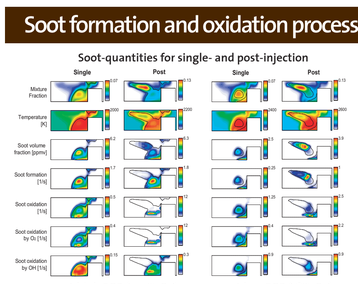

at high EGR (12.5% O2) at low EGR (18% O2)

Soot evolution at low EGR (18% O2)

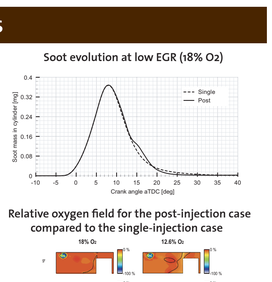

Relative oxygen field for the post-injection case compared to the single-injection case

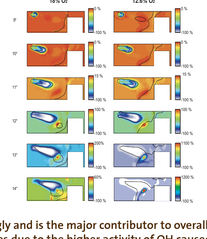

Enhancement of soot oxidation rate
- order of magnitude enhancement at high EGR (larger soot volume)
- caused by additional locally available oxygen
- soot evolution of the low-EGR case shows an initial increase due to added fuel, but subsequent drop due to improved oxidation

O2 difference (normalised by the O2 distribution of the single-injection case) shows an accumulation of O2 at the tip of the post-injection being pushed into the main flame.

At low ambient oxygen levels, the oxidation rate by O2 is found to rise strongly and is the major contributor to overall oxidation. At high ambient oxygen the contribution of O2-oxidation decreases due to the higher activity of OH caused by the increase in flame temperature.

Engine heat release and flowfield validation

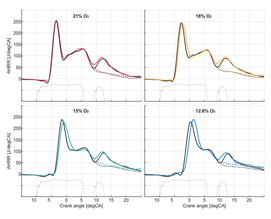

- very good accuracy maintained considering the large dilution spread
- overestimations of AHRR of the main injection strongly influence the ignition and heat release from the ‹sensitive› post-injection
- excellent prediction of the position of the post-injection soot with respect to penetration and orientation
- impingement on the wall and subsequent curling qualitatively well captured

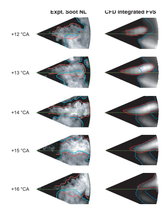

Soot formation and oxidation processes

[1] O'Connor, J. and M. Musculus. *International Journal of Engine Research*, 2013.
[2] CD-adapco, STAR-CD v4.16, 2010.
[3] A. Y. Klimenko and R. W. Bilger. *Progress in Energy and Combustion Science*, vol. 25, pp. 595-687, 1999.
[4] Y. M. Wright, et al. *Combustion and Flame*, vol. 143, pp. 402-419, 2005.
[5] S. L. Liu, et al., *Combustion and Flame*, vol. 137, pp. 320-339, 2004.
[6] K. M. Leung, et al. *Combustion and Flame*, vol. 87, pp. 289-305, 1991.
[7] J. F. Widmann. *Combustion Science and Technology*, vol. 175, pp. 2299-2308, 2003.
[8] Bolla, M., et al. *International Multidimensional Engine Modeling Users' Group Meeting* 2014

Acknowledgements

Funding
- Competence Center for Energy and Mobility (CCEM-CH) project "In-cylinder emission reduction for large diesel engines"
- Swiss Federal Office of Energy (BfE)

Pandurangi, Frapolli, Bolla, Boulouchos & Wright. Influence of EGR on Post-Injection Effectiveness in a Heavy-Duty Diesel Engine Fuelled with n-Heptane. SAE 2014-01-2633.

M. Schmitt martin.Schmitt@lav.mavt.ethz.ch
C. E. Frouzakis frouzakis@lav.mavt.ethz.ch
Y. M. Wright wright@lav.mavt.ethz.ch
K. Boulouchos boulouchos@lav.mavt.ethz.ch

DNS IN ENGINE-LIKE GEOMETRIES

Introduction

Internal combustion engine flows are turbulent, unsteady and exhibit high cycle-to-cycle variations. There are multiple turbulence generating mechanisms and their effects overlap in time and space, creating strong challenges for the turbulence models currently used.
In this project, the flow in engine-like geometries is investigated using Direct Numerical Simulation (DNS), high-fidelity numerical experiments with high temporal and spatial resolution. The results can be used for better understanding of in-cylinder processes and for model validation purposes.

Simulation Setup

Boundary Condition (BC):
- Dirichlet Boundaries for velocity and Temperature
- The piston moves according to a harmonic function according to the piston speed of 200/560 rpm
- Compression ratio = 12 (compression)

Simulation data:
- 160,000 CPUh / cycle (flow)
- 200,000 CPUh / compression
- 15 TB raw of data
- 8 flow cycles / 8 compressed cycles

Grid:
- 70 - 100 million grid points
- Grid generation: Cubit

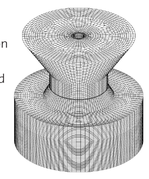

Numerical Tool

- Spectral element discretization based on the incompressible flow solver *nek5000*
- High-order fluid/thermochemistry splitting (low Mach number formulation)
- Implicit integration of thermochemistry
- Implicit/explicit integration of hydrodynamics
- Detailed chemical kinetics and transport
- High scalability / parallel efficiency

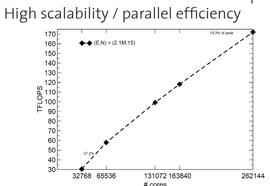

Extreme scaling workshop, 2010 Jülich BG/P (S. Kerkemeier et al., Techn. Report, Jülich Supercomputer Center 2010)

Experiment

LDA meassurements by Morse, Whitelaw and Yianneskis (1979)

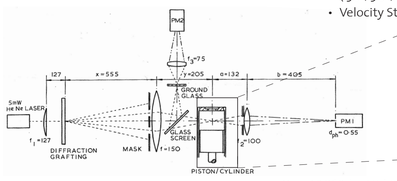

Available data:
- Mean and rms velocity field at four times (36°, 90°, 144° and 270°CA)
- Velocity Streamlines

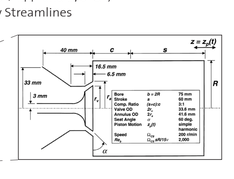

Morse, A.P., Whitelaw, J. H. & Yianneskis, M. 1979 Turbulent flow measurements by laser-doppler anemometry in motored piston-cylinder assemblies. J. Fluids Eng. 101, 208–216.

Governing equations

Continuity:

$$\frac{\partial \rho}{\partial t} + \nabla(\rho \vec{u}) = 0$$

Momentum in a moving reference system (ALE):

$$\rho\left(\frac{\partial \vec{u}}{\partial t} + (\vec{u} - \vec{w}) \nabla \vec{u}\right) = -\nabla p_1 + \nabla \cdot (\mu \bar{S})$$

Energy in a moving reference system (ALE):

$$\rho c_p \left(\frac{\partial T}{\partial t} + (\vec{u} - \vec{w}) \cdot \nabla T\right) = \nabla \cdot \lambda \nabla T + \sum_{i=1}^{N} h_i^0 \dot{w}_i - \nabla \cdot \rho T \sum_{i=1}^{N} c_{p,i} Y_i \mathbf{V}_i + \frac{\partial p_0}{\partial t}$$

Cycle to Cycle Variations

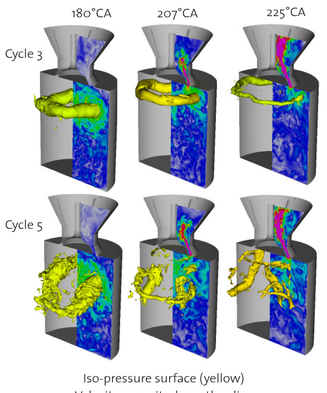

Iso-pressure surface (yellow)
Velocity magnitude on the slice

Intake Stroke

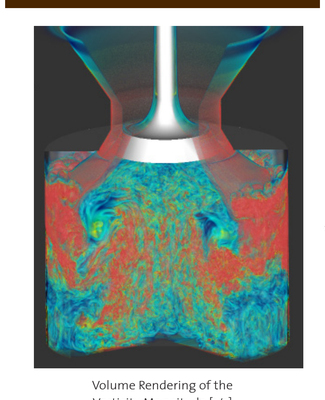

Volume Rendering of the Vorticity Magnitude [1/s]

Temperature & Flow at TDC

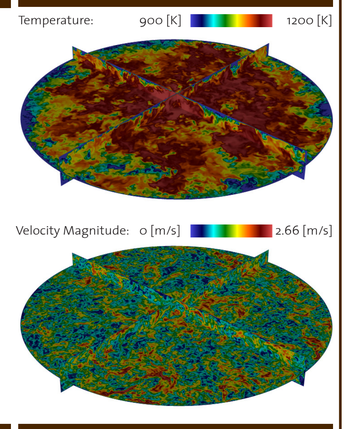

Wall Heat Losses

Heat flux through the cylinder head [W/m²]

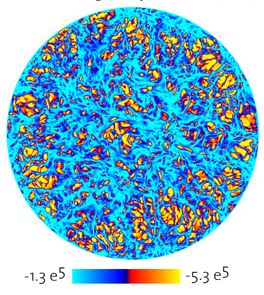

Wall normal velocity close to the cylinder head [m/s]

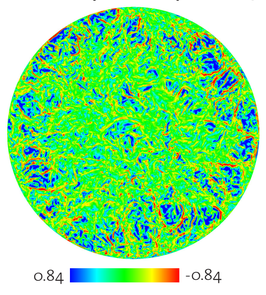

Future Work

- Investigate auto- and forced ignition and flameflow interactions
- Effects of cycle-to-cycle Fluctuations in the HCCI combustion mode
- Detailed Investigation of Wall Heat Losses during compression and later combustion
- Simulate more realistic engine geometries

Acknowledgements

- Financial support: SNF 200021_135514
- Computational resources:
  - Swiss National Supercomputing Center (CSCS)
  - ETHZ HPC Cluster brutus
- Visualization: Jean Favre, CSCS
- Ananias Tomboulides, Univ. W. Macedonia, Greece